POLITECNICO DI TORINO
Repository ISTITUZIONALE

Designing 3D printable polypropylene: Material and process optimisation through rheology

(Article begins on next page)

01 September 2025

Designing 3D printable polypropylene: material and process optimisation through rheology.

M. Bertolino*, D. Battegazzore, R. Arrigo, A. Frache*

Dipartimento di Scienza Applicata e Tecnologia
Politecnico di Torino, Alessandria Site, V.le Teresa Michel 5, 15121, Alessandria, Italy

Corresponding authors.
Email address: michele.bertolino@polito.it; alberto.frache@polito.it;

Abstract

A polypropylene-based material has been formulated to be suitable for fused deposition modelling (FDM). In fact, the high volumetric shrinkage and the rheological behaviour are main problems whereby polypropylene (PP) is not commonly used as a 3D printing filament. Experimental results have evidenced how material modifications have a strong impact on rheological behaviour, providing critical features that permit and improve material printability. An optimised 20 wt.% talc filled heterophasic PP copolymer has been developed. The peculiar properties of the materials have been assessed by thermal characterisation and rheological analysis. Several process parameters (extrusion temperature, screw speed, cooling conditions) have been evaluated in order to obtain a proper filament. Finally, a model part has been printed using different settings to check printing quality by morphological analysis.

1. Introduction

Among all the 3D printing techniques for polymers fabrication [1, 2], Fused Deposition Modelling (FDM) is the most used and the most developed in the global production system [3], being simple and economic in terms of both materials and tools. Known alternatively as Fused Filament Fabrication (FFF), because of the lack of a precise standardization in the additive manufacturing world [4, 5], this technique "prints" an object in its final shape layer by layer, depositing the material through a nozzle fed with a proper filament.

Frequently, the limiting factor for additive manufacturing is just the scarce list of available material [6-10]. The common polymers for FDM available on the market are few, such as PLA, Nylon, ABS or PC, and most of all with almost no specific functionalization. In the last years, scientific world has become aware of this gap and some studies have been carried on to investigate the behaviour of more performing polymer-based composite [11], reinforced with natural and synthetic fillers [12-15], and new high performance filament such as PEEK [16] or PEI (ULTEM®) [17]. In this process of enhancement, Duty et al. tried to develop a practical model to evaluate polymers as candidates for extrusion-based additive manufacturing, outlining some specific conditions that a material must fulfil in its flow during extrusion and in its stability after been deposited [18]. Nevertheless, the problem is that there is still the absence of a deep knowledge of the specific properties that a material should have to be 3D printable, so that the know-how is closed and protected by the industrial suppliers. From the 80ies, the market of 3D printing technologies has risen and spread in many sectors, such as biomedical, automotive and aerospace, and the tendency is now to enlarge it up to buildings, electronics and design [19, 20]. The greatest advantage of additive manufacturing is the complete independency on the final shape of the product, which is entirely customizable with approximatively no costs, and therefore the widest materials portfolio is necessary to level up the applications of this technology [21, 22].

With all this in mind, the driving force of this work has been to develop a deeper knowledge about polypropylene (PP), one of the most studied and commercialised polymer in the world, focusing on the features that it must have to be suitable for FDM. This polymer is now becoming available as filament for 3D printing, but only few studies have been conducted on the characteristics of a 3D printing grade [23-25].

The reasons why pure PP is difficult to process with FDM technology and must be modified with other polymers and fillers are directly connected with its volumetric shrinkage and rheology.

Volumetric shrinkage and the severe warpage that it can induce on the printed object are well-known and studied problems of all semi-crystalline thermoplastics [26], and most of all of PP [27], which generally has an high crystallinity grade, due to the isotactic macromolecular structure in which it is usually synthesized [28, 29]. This defect is strongly dependent on the printing object's shape: the greater the size is, the more impactful the deformation will be. Moreover, one dimension much greater than the other two leads to an evident warpage and if the dimensions are almost equal, like a cube, a shrink-mark on the surfaces will appear. This negative feature of PP must be minimized to obtain a good quality 3D printed object, even if for very small objects the adhesion to the printing bed alone may be sufficient. With this in mind, PP can easily and successfully blended or copolymerised with other polymers, in order to decrease crystallinity and so volumetric shrinkage related problems [30-32]. For example Jin et al. tried successfully to reduce 3D printing warpages of polypropylene/ethylene random copolymers by adding various amorphous PPs and also demonstrated that LLDPE instead has almost no effect on PP crystallinity [25]. In addition, Wang et al. developed a model to evaluate warpages during FDM process, basing on several factors [33]. Other studies have been conducted coupling the copolymerisation effect with fillers, to reduce the volumetric shrinkage and in parallel enhance the mechanical properties. For example Spoerk et al. managed to reduce warpages by introducing expanded spherical perlite particles in a PP copolymer [12].

While for the printing process volumetric shrinkage is widely recognised as an issue, it is not generally considered in the filament making process. Theoretically, the ideal filament for 3D printing has a perfect smooth surface, a precise circular cross-section, a constant diameter and, most of all, each of these properties must replicate all over the filament. The problem is here that a differential shrinkage in the cooling direction can occur and lead to an oval cross-section. As the 3D printer expect a circular filament, this imperfection can cause problems during the printing stage, such as inhomogeneous deposition due to singularity in the material flow at the extrusion nozzle, blocks of the pulling system of the printer and nozzle clogging.

Concerning now rheology, more issues can be then correlated to this fundamental polymer property [34, 35]. We would like to focus the attention on how deeply understand the rheological characteristics of a polymer is mandatory to determine if it can be processed by FDM or not and then to optimise the object final quality.

First of all, pure PP has a typical Newtonian behaviour at low shear rates, with a large plateau reaching the zero frequency value. This is a problem when this condition occurs in the process, e.g. during the not printing extruder movements or when it temporarily stops, so that the absence of a yield stress behaviour cause material oozing. Another zero-shear condition is obviously when the material is deposited, when it is still in the semisolid state. In this case, a high value of yield stress together with a strong shear thinning behaviour would assure the material to keep its shape without drooping [36]. The second problem related to rheology is filament buckling, which cause the inability to deposit the material. This phenomenon occurs if the pressure applied by the rollers to drive the filament through the nozzle is greater than a critical stress [37]. This stress is directly related to the compressive modulus of the material and the *slanderness ratio* of the filament L/R, where R is the filament radius and L is the length of the filament that withstands the rollers pressure. Since this pressure is found to be proportional to viscosity [34, 37], as will be explained later, it results that a too high viscosity must be avoided. This statement clashes with the filament making process, where a high viscosity is

helpful, so that a compromise must be found. The third and last problem concerning rheology is die swelling, which increases again with the applied pressure and affects print resolution.

Finally, a further particular problem working with PP is that it shows a very low adhesion to every other material. This fact, combined with the shrinkage, makes necessary the use of a PP printing surface, or at least a PP layer on the bed to promote adhesion. UHMW-PE has been found to be also a good substrate. [38]

In order to achieve a deeper knowledge, in the first part of this work PP-based compounds have been studied, investigating their thermal and rheological properties related to FDM. In the second part, a step-by-step optimisation of the process parameters has been conducted, outlining some general rules and suggestions to fulfil the FDM filament requirements and to improve the details resolution of a 3D printed little model.

2. Materials and Methods

2.1. Materials and methods

Different grades of PP have been used. *Table 1* resumes the commercial and supplier names, the melt flow index (MFI) as reported on the technical datasheets and the codes used in the text. In the same table a commercial composite based on PP and containing 40 wt.% of talc (coded as PP HOMO TALC) is reported.

Table 1. Specifications of the commercial materials.

Commercial name	Supplier	Density [g/cm^3]	MFI	Code
PP PPH 1060	Total – Polymers	0.905	0.3	PP HOMO 0.3
ISPLEN PP 070 G2M	Repsol – Chemicals	0.905	12	PP HOMO 12
Axtroplen TC4	Arcoplex Trading	1.23	14	PP HOMO TALC
ISPLEN PB 170 G2M	Repsol – Chemicals	0.905	12	PP COPO 12

In addition to the commercial formulations, PP COPO 12 has been melt-compounded with 20 wt.% of talc IMI FABI HTP1 in the twin screw extruder LEISTRITZ ZSE 18/40 D equipped with a gravimetric feeder (details in *Figure 1(a)*). In this process, the screw speed has been set to 350 rpm and the material feed rate to 1.5 kg/h, resulting in a residence time of about 100 s. The obtained composite has been coded as PP COPO TALC. Talc IMI FABI HTP1 grade was supplied by IMI FABI SpA and its main properties are: D_{50}=1.9 µm, D_{98}=8.0 µm; density 2.8 g/cm^3 and specific surface area (SSA) 10 m^2/g.
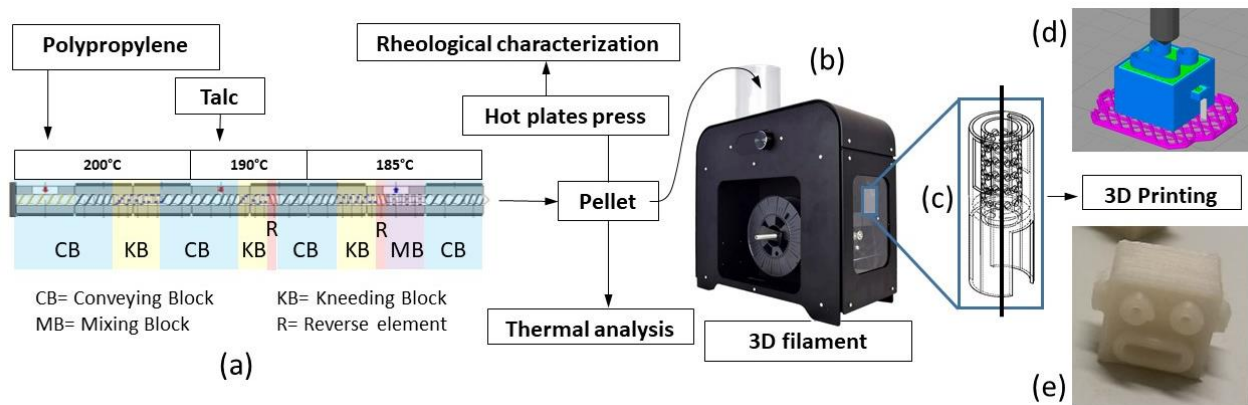
Figure 1. Working Scheme: (a) Twin screw compounding process details; (b) Filament making machine; (c) Homemade 3D printed airflow deviator; (d) 3D Printing software design project; (e) Final 3D printed object.

The compounded and neat pellets have been shaped in the form of disks (25 mm diameter for 1 mm thickness) as a suitable specimen for the rheological analysis (*Figure 1*). The operation has been carried out by pressing the pellets at 100 bar into a right-shaped metallic mould, heated at 210°C, for 3 minutes by using a hot plates press Collin P 200 T.

The thermal analysis was performed directly on the neat or compounded pellets.

2.2. 3D Printing equipment

Next 1.0 Advanced filament making machine by 3Devo (*Figure 1(b)*) has been used to produce a filament with a nominal diameter of 1.75 mm. This machine is composed of a single-screw extruder with four heating stages, an air cooling system composed of two fans, two rollers that pull the extruded material and a filament rolling system on a spool. The speed of the rollers is controlled by a system that in-line gauge the filament diameter with a laser and automatically adjust the speed in order to maintain it at the set value. However, this automatic process is not enough for PP based materials. Indeed, to solve the problem of differential shrinkage due to the directional flow of the two cooling fans, according to the supplier indications, a homemade flow deviator was 3D printed (*Figure*

1(c)). This add-on has been placed between the two fans and the filament passes through it, making the cooling more homogeneous.

Roboze One 3D printer has been used. It is a traditional open-chamber FDM machine, with a printing plate of 28 cm x 34 cm equipped with a 0.4 mm nozzle.

As PP shows serious issue to adhere to any surface, the 3D printer bed was fully covered with two different scotch tapes: the first one can survive to high temperature and adheres to the metal plate, while the second one made of PP adheres to the first one and matches perfectly with the deposited material.

Simplify 3D and Solidworks 2018 software have been used to set the parameters of the 3D printer machine and to CAD design the parts (*Figure 1(d)*), respectively.

2.3. Characterization techniques

2.3.1. Differential Scanning Calorimetry

Thermal properties have been evaluated by Differential Scanning Calorimetry (DSC), using a DSC Q20 supplied by TA Instruments. Each sample of 7 ± 1 mg was put into a chamber purged by nitrogen at 50 mL/min and was firstly heated from -50°C to 220°C at 10°C/min in order to erase the previous thermal history. Therefore, after a 2 min isothermal step at 220°C, the sample was cooled at 10°C/min back to -50°C and finally reheated up to 220°C by a ramp of 10°C/min. The information achieved by this analysis are: Crystallization temperature (T_c), evaluated as the endothermal peak maximum abscissa of the heat flow during the cooling cycle; Melting temperature (T_m), evaluated as the exothermal peak maximum abscissa of the heat flow during the second heating cycle; Melting Enthalpy (ΔH_m), evaluated as the area under the exothermal peak of the heat flow during the second heating cycle. To calculate the crystallinity percentage (X_C) of the PP-based pellets, the following formula has been used:

8

$$X_C = \frac{\Delta H_m}{\Delta H_{100}(1-x)} \tag{1}$$

where ΔH_m is the melt crystallization enthalpy obtained from the second heating scan, ΔH_{100} represents the melting enthalpy of the 100% crystalline polymer and x is the filler weight fraction. The value of 207 J g^{-1} has been considered as a reference for the 100% crystalline PP melting enthalpy [39]. Because of the wide crystallization range, each ΔH_m has been calculated by integrate the exothermal peak from 100°C to 185°C, using the Universal TA software.

2.3.2. Rheological analysis

Rheological properties of the different PP grades and the PP-based compounds have been evaluated using an ARES (TA Instrument, USA) strain-controlled rheometer in parallel plate geometry (plate diameter: 25 mm). Preliminary strain sweep tests were carried out at 190 °C and $\omega = 100$ rad/s. The complex viscosity and storage and loss moduli were measured performing frequency scans from 10^2 to 10^{-1} rad/s at different temperatures. The strain amplitude was selected for each sample in order to fall in the linear viscoelastic region (an example is reported in *Figure S1*).

2.3.3. Morphology

The surface morphology of filaments and the details resolution of 3D printed objects were investigated using a Scanning Electron Microscope (SEM) Zeiss LEO-1450VP by Zeiss (beam voltage: 20 kV; working distance: 15 mm). The surfaces were directly investigated by cutting small pieces. All the surfaces were covered by a gold layer with Gold Sputter Coater – Emitech K550.

3. Results and discussion

3.1.1. Rheological Characterization

In order to have a screening of rheological behaviour of different PP grades, characterized by different MFI or by the presence of another polymer or a filler, viscosity curves at different temperature of all selected material were obtained (*Figure 2*). Since the recommended printing temperature of PP is about 260°C, the analysis at this temperature is expected to be the most important, because it describes the rheological behaviour of the material during the printing stage. However, in order to optimize the processing conditions in the filament making and the printing processes, the rheological characterization was carried out also at different temperature values.

Since from the first analyses at 190°C it is clear that the filler introduction modifies the rheological behaviour of polypropylene. In fact, one can clearly see how PP HOMO 12, a neat PP, shows a typical homopolymer-like behaviour, with a Newtonian plateau in the low frequency range, which evolves in a shear thinning behaviour as the frequency increases. As expected, PP HOMO 0.3, characterized by a lower MFI, exhibits higher viscosity values than PP HOMO 12, about thirty times more at 0.1 rad/s, and a more evident shear thinning behaviour. The introduction of talc particles significantly modifies the rheological behaviour of PP; in fact, PP HOMO TALC does not show the Newtonian plateau at low frequencies, and a well-pronounced yield stress can be observed in the range of 1-10 rad/s. This behaviour can be attributed to the well-dispersed talc particles throughout the PP matrix, causing a restrain of the relaxation dynamics of PP macromolecules with a consequent increase of the complex viscosity values. [40, 41]

The presence of a second polymer in the matrix seems to have a negligible effect on the polymer rheological behaviour both at 190°C and at 210°C, because the curves of PP COPO 12 almost overlap those of PP HOMO 12. This fact could be expected, since the value of MFI of the two systems is the

same. Differently, at higher temperatures, the effect of the second phase is more evident, with the appearance of a yield stress behaviour in the low frequency range.

Finally, coupling the talc and the second polymer effects, PP COPO TALC curve shows a pronounced yield stress at low frequencies, followed by a shear thinning behaviour. These effects are more evident at 230°C, with the obtainment of higher values of complex viscosity, and become critical at 260°C, where the curve shows a tremendous yield stress behaviour approaching 0.1 rad/s. This strong yield stress behaviour is the consequence of an optimal distribution and dispersion of the talc particle in the material (SEM images of the filament section are reported in *Figure S2*). We remind that this behaviour is particularly recommended for FDM 3D printing, because it allows the material to be stable from a rheological point of view when deposited and therefore to maintain its shape. The yield stress values for each material has been calculated using the Carreau-Yasuda model and can be found in the supplementary material (*Figure S3, Table S1*).

It is noticeable to highlight that all these effects become more and more evident by increasing the temperature: the improved mobility of the polymer chains at higher temperature allows the motion of the fillers, which are able to organize in complex structures strongly affecting the material rheological behaviour [42, 43]. The opposite effects of temperature, which tends to decrease viscosity, and filler, which if activated is capable to increase it, can be seen comparing the temperature evolution curves of PP HOMO MFI 12 and PP HOMO TALC (*Figure 3*). While for the first pure PP the curves are almost parallel and simply shifted to lower values of viscosity, the talc in the second polymer invert the tendency: at 260°C the rheological curve is higher than the one at 230°C and the viscosity value at 0.1 rad/s is even equal to one obtained at 190°C.
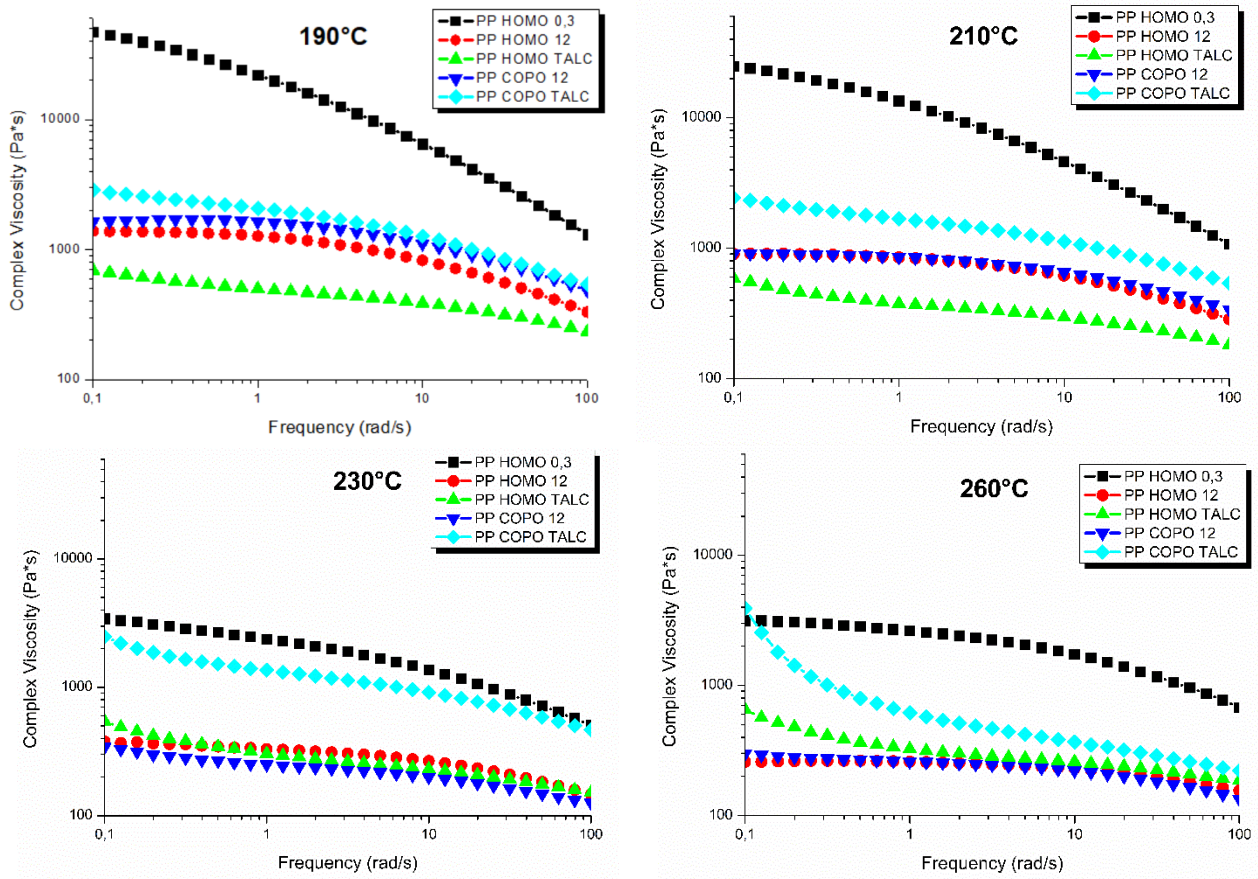
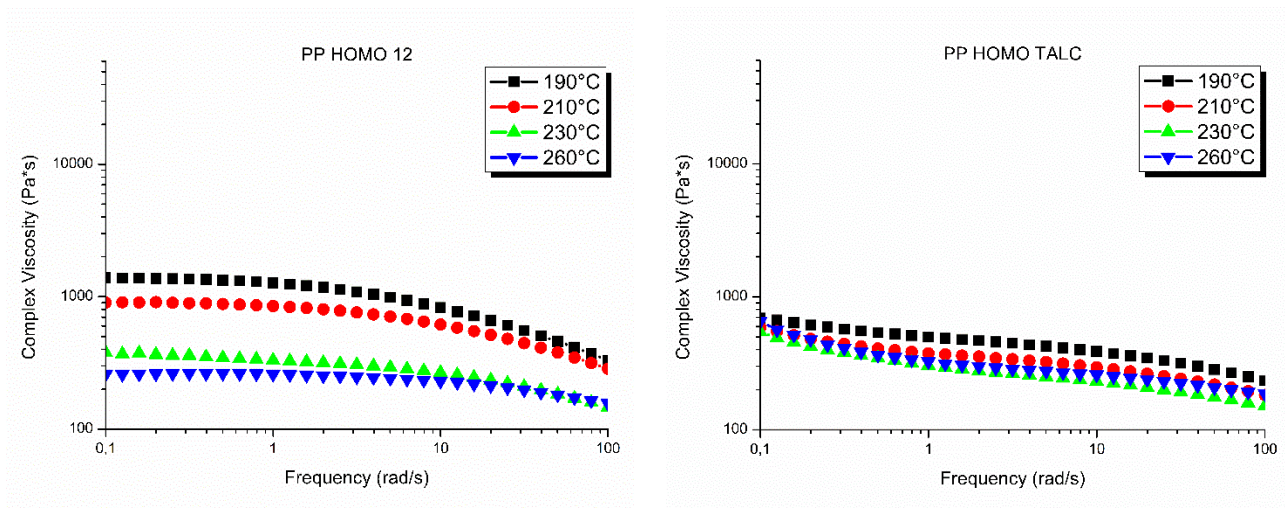*Figure 2. Rheological curves of different PP grades, compared at different temperatures.*

Figure 3. Rheological curves of PP HOMO 12 and PP HOMO TALC, compared at different temperatures.

12

Regarding the 3D deposition process, one can calculate the value of shear rate that the material must bear when it passes through the nozzle, using the following equations [34, 37]:

$$\dot{\gamma}_{app} = \frac{32Q}{\pi d_n^3}\left(\frac{3n+1}{4n}\right) \tag{2}$$

$$Q = \frac{\pi d_f^2 v}{4} \tag{3}$$

where $\dot{\gamma}_{app}$ is the apparent shear rate, d_n is the nozzle diameter, d_f is the filament diameter, v is the printing speed, Q is the material flow and n is the pseudoplasticity index. Setting default parameters (such as 50 mm/s, 1.75 mm and 0.4 mm) and using the pseudoplasticy index of PP COPO TALC, calculated with Carreau-Yasuda model (*Table S1*), the shear rate is typically in the order of 10^3 to 10^4 s^{-1}, a range that is above the attainable shear rate performed by a rotational rheometer. However, since at high shear rates the rheological behaviour is governed by the matrix, the complex viscosity values of the different materials would be similar.

3.1.2. Thermal Characterization

DSC analyses have been performed to measure the ΔH_m and X_C, which are both values correlated with the volumetric shrinkage of the material (main data reported in *Table 2*).

The melting temperature is slightly affected by the viscosity of the polymer as well as by the filler presence. PP COPO 12 has one single endothermal peak at 165°C, that shows how the material is not a blend. Moreover, PP is the predominant polymer, so that the melting temperature is not affected by the second material used. This material seems coherent with the *heterophasic copolymer* definition given by Gahleitner et al. [32].

Pursuing the data analysis obtained from the DSC, the effect of adding talc on the polymer crystallinity (X_C) and crystallization temperature (T_c) is the most evident result. By adding talc, the polymer crystallisation is promoted, so that T_c increases. This is due to the fact that introducing a

second phase in a polymer leads to heterogeneous nucleation of polymer crystalline domains, which is faster and requires less activation energy [44]. On the other hand, inorganic fillers are well known additives to be used in order to increase the dimensional stability of injection molded parts [45, 46]. Indeed, even if X_C slightly increases or remains comparable, such as for PP COPO TALC, the shrinkage of the material could be reduced by the inorganic and no deformable part. For this reason, the enthalpy (ΔH_m) have to be considered for this evaluation, because it reflects the overall shrinkage behavior of the material. By this way, the two formulations with the inorganic filler have the lowest ΔH_m with a difference between them that is only due to the talc content.

Table 2. Scanning calorimetry data of the materials.

PP code	T_c [°C]	T_m [°C]	ΔH_m [J g^{-1}]	X_c
HOMO 0.3	111	169	102	49
HOMO 12	113	165	91	44
HOMO TALC	126	164	66	53
COPO 12	114	165	96	46
COPO TALC	126	166	74	45

3.2. Filament making optimisation

Relying on direct observation of the solidified filament and especially of the material flow through the extruder nozzle, several trials have been carried out for each PP in order to obtain the best possible filament. The evaluated parameters, collected in *Table 3*, were the heaters temperature (*H* followed by a number, from the feeder to the die) of the device, the screw speed (*n*) and the working percentage of the cooling fans.

Looking at the viscosity curve and the melting temperature obtained previously, the right process temperatures are chosen and then optimised. Hence, the screw speed is taken to the minimum value

of 2 rpm and then increased gradually until the diameter control remains acceptable, increasing the fan speed in order to faster solidify the material. As expected, it has been observed that a strong cooling is deleterious for the filament cross section, which tend to become oval as the fan speed is increased. It seems to be clear that a compromise between the parameters needs to be accepted in order to realize the best filament possible.

Table 3. Results of the filament making optimisation for each PP grade.

Material	H1 - H2 - H3 - H4 [°C]	n [rpm]	fan speed [%]
PP HOMO 0.3	190 – 185 – 185 – 180	5	50
PP HOMO 12	190 – 180 – 180 – 170	2	20
PP HOMO TALC	180 – 175 – 175 – 170	2	20
PP COPO 12	190 – 180 – 180 – 175	2.5	30

A deeper study was performed with the more promising material, which was found to be PP COPO TALC. For this material, the surface finish has been improved by increasing the temperatures above 200°C, reducing the screw speed to maintain diameter stability. The filament quality was evaluated by observing surface roughness directly using Scanning Electron Microscopy. In *Table 4* are reported the two possible configuration for this material: *Method 1* allows to faster filament production, while *Method 2* decrease sensibly surface roughness, as can be seen by the SEM images in *Figure 4*. Comparing the images on the left, it is clear how the surface become smoother increasing the temperature (*Method 2*). With a higher magnitude (right images) striping defects of about 10 µm can be identified on the entire surface, while in the lower image (*Method 2*) only spot defects of 5-10 µm are present.

Table 4. Two possible configurations for the filament making process of PP COPO TALC.

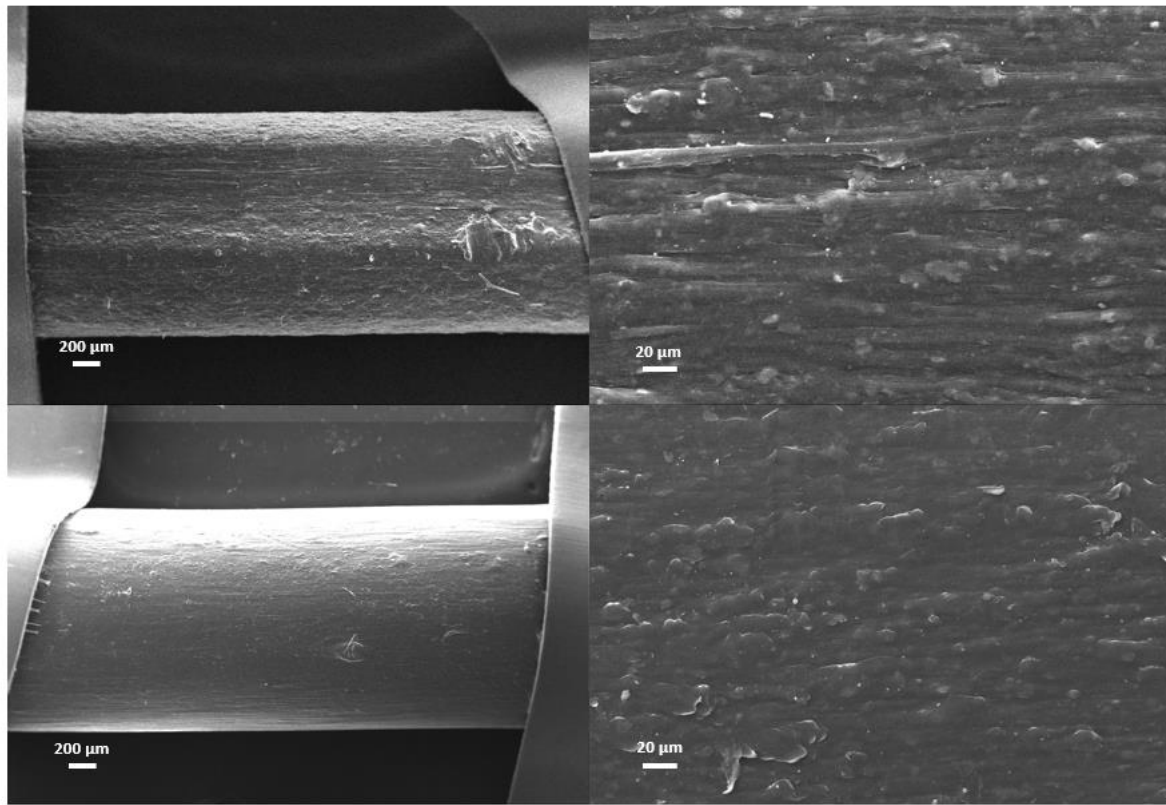| Method n°	H1 - H2 - H3 - H4 [°C]	n [rpm]	fan speed [%]
1	190 – 185 – 185 – 185	4.5	40

Figure 4. SEM images of the surface of different filaments. Top: method 1; bottom: method 2.

The problem of oval cross section, which makes the diameter value dual, corresponding to the major and minor axes of the ellipsoid (respectively D_1 and D_2 in *Table 5*), was analysed for all the material, since it is an important quality indicator. In particular, the major corresponds to the direction of the laser dimensional scanner, while the minor to the perpendicular direction, the one affected by directional shrinkage. $D_{1,av}$ and $D_{2,av}$ are the average values of a series of diameter measurements on each filament, with a distance of 10 cm for a length of 2 m. Since the target value is 1.75 mm, it is clear how adding talc in a PP heterophasic copolymer seems to be the better choice in order to obtain a good filament for FDM 3D printing. Both the oval cross section problem and the diameter constancy (standard deviation) are enhanced by modifying a neat PP in such a way. In *Table 5* all the average diameter measurements are resumed, with the related standard deviation; for each material, the ovality

corresponds to the difference between $D_{1,av}$ and $D_{2,av}$. The precise measurements for each filament can be found in *Figure S4, S5, S6, S7, S8* in supplementary material.

Table 5. Average filament diameter measurement and the relative standard deviation.

PP code	$D_{1,av}$ [mm]	ST.DEV. [mm]	$D_{2,av}$ [mm]	ST.DEV. [mm]	Ovality [mm]
HOMO 0.3	1.76	0.05	1.51	0.04	0.25
HOMO 12	1.81	0.05	1.22	0.04	0.59
COPO 12	1.90	0.14	1.48	0.13	0.48
HOMO TALC	1.92	0.10	1.74	0.10	0.18
COPO TALC	1.73	0.03	1.68	0.02	0.05

3.3. FDM 3D printing optimisation

As for the filament making, parameters optimisation trials have been carried out also for 3D printing. The quality assessment took into account specific observations, such as compliance with the dimensions, definition of details, warpage and the occurrence of adhesion problems between the layers.

The object of study was designed using the CAD software as a little robot-head (*Figure 5*). From a geometrical point of view, this object is a squared parallelepiped, with an edge of 10 mm and height of 8 mm. The "face" is made by two hollow cylinders, with inner diameter of 1.5 mm and outer of 3 mm, the "mouth" is made with the same two semi circles connected by rectilinear parts to make a slotted hole protruding 1.5 mm. The "ears" are parallelepiped of dimensions 1 x 3 x 1.5 mm^3, positioned onto opposite faces. All of these details have been added to evaluate the printing and the support structures accuracy.

Figure 5. Robot-heads used as model parts for the printing tests.

During the various steps, some settings have been kept unchanged, such as the infill percentage of 20%, the deposition pattern as ±45°, the extrusion width of 0.4 mm, the layer thickness of 0.2 mm and the bed temperature at 80°C, while the optimisation has been focused on the printing temperature and speed. The process parameters and some qualitative evaluations on the material behaviour are reported in *Table 6*.

Table 6. Process parameters of 3D printing and process qualitative evaluations. Filament buckling refers to material flow instability, which prevent 3D printing. Printability is achieved if the model can be successfully printed. Final quality is evaluated in terms of dimensions, definition of details, warpage and the occurrence of adhesion problems between the layers.

PP code	Temperature [°C]	Speed [mm/s]	Filament Buckling	Printability	Final quality
HOMO 0.3	250	60	✓	χ	-
HOMO 12	220	60	χ	χ	-
COPO 12	230	60	χ	✓	Poor
HOMO TALC	230	60	χ	✓	Poor
COPO TALC	250, 210	60, 30	χ	✓	High

A first trial has been done looking at how the material exits from the 3D printer nozzle. The right temperature for each material was chosen as the maximum temperature in order not to have material

drooping from the nozzle when the 3D printer is not working. At this temperature, specific for each PP grade and reported in *Table 6*, all the materials flows were smooth and suitable for 3D printing, except for PP HOMO 0.3. In this case, the filament showed flux instability, with a "curly" extruded filament, due to filament buckling through the nozzle (*Figure S9*). This phenomenon could be expected looking at the rheological curve (Figure 2), following the rheological issues explained in the introduction, which already suggested problems with too viscous polymers. In particular, the pressure applied ΔP on the filament can be related to viscosity and the critical buckling stress σ_{cr} to the compressive modulus with the following equations [37]:

$$\Delta P = \frac{8 Q \eta_a l}{\pi r^4} \tag{4}$$

$$\sigma_{cr} = \frac{K \pi^2}{\left(\frac{L}{R}\right)^2} \tag{5}$$

where l is the dimension of the nozzle, η_a is the apparent viscosity, r the nozzle radius, Q the material flow during the extrusion (equation (3)), K the compressive modulus of the material and L/R the slenderness ratio of the filament. Keeping constant all the geometrical and process parameters and reminding that buckling occurs if applied pressure exceeds critical buckling stress, the decisive factors become viscosity and compressive modulus. Since different grades of neat PP would have comparable compressive modulus, it results that the problem is the too high viscosity of this PP grade, which generates a high pressure that cause filament buckling and totally preclude the possibility to 3D print the material, as the deposited filament broke continuously and was not able to follow the pattern. Therefore, with the parameters used PP HOMO 0.3 resulted unprintable.

The printing stage was then performed with all the other materials, with a speed of 60 mm/s. The trial with PP HOMO 12 was not successful: due to the low viscosity and the absence of yield stress behaviour, the filament was not able to follow the pattern at this speed. A robot-head made by PP

COPO 12 and PP HOMO TALC was instead built, but for the first formulation, the volumetric shrinkage prevented a good final quality, while the low viscosity of the second one did not allow to reach a high detail resolution (SEM images in *Figure S10*).

Again, the most performing solution seems to be PP COPO TALC and a deeper analysis trying to improve the final quality was performed. This optimisation can be seen in *Figure 6*, and revealed how printing temperature and speed are closely correlated: higher printing speeds require higher temperatures (*Table 7*). In addition, the higher the speed is, the lower the detail resolution will be, but a speed too low is negative for edge warpages, because a layer is not quickly reheated as the upper layer is deposited and the material has more time to shrink. This type of warpages is due to the high differential volumetric shrinkage of PP, and reducing the distance between the nozzle and the bed temperatures has the more positive effect in order to reduce it. Also a printing temperature too low can have a negative influence, causing less adhesion between each layer and the appearance of holes on the object surface, as can be seen in the right-centred image of *Figure 6*.

As a last consideration, it must be said that this settings worked on a model of limited size. For bigger objects other problems may occur, especially concerning warpages. One more problem dealing with an object of greater dimensions could be a "pulling" effect on the deposited filament: if the material is not fluid enough, a high printing speed makes the nozzle pull the deposited filament, which become thinner, and this changes a lot the extrusion width and consequently the layer adhesion.

Table 7. Three possible configurations for the 3D printing process of PP COPO TALC.

Method n°	Nozzle Temperature [°C]	Printing Speed [mm/s]
1	250	30
2	250	60
3	210	30
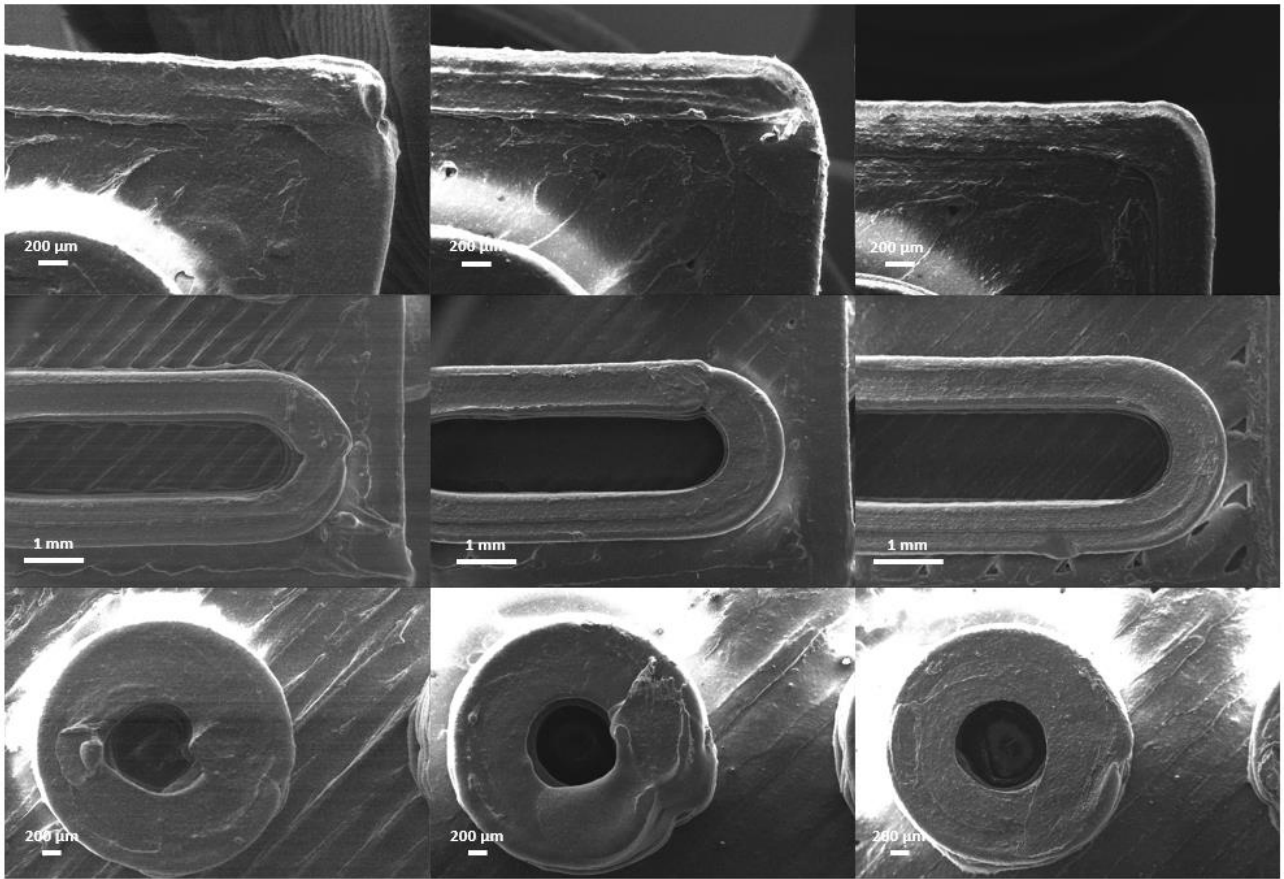
Figure 6. SEM magnifications of three different robot's heads obtained with different parameters applied on PP COPO TALC. Left: method 1; middle: method 2; right: method 3 reported in Table 7.

4. Conclusion

A PP-based compound suitable for FDM technique has been formulated and optimised. The features have been identified and their achievement has been investigated through thermal and rheological analysis. Furthermore, the right parameters of the filament making process have been optimised and the effect of the printing parameters on the quality of a specific model has been studied.

The results obtained are summarized as follow:

- The main issue to overcome is the high volumetric shrinkage of PP. To fulfil this requirement, the enthalpy of the material must be minimized. A successful solution is the addition of an inorganic filler, such as talc.

- A non-Newtonian behaviour at low shear rate values, showing a strong shear thinning effect, is fundamental at the temperature used in the FDM technique. Once again, the presence of talc has been found to be a good solution. Moreover, the yield stress behaviour of the rheological curve is enhanced by the copolymerization of the matrix.

- High viscosity can cause filament buckling during the deposition process of FDM, resulting in the complete non-printability of the material.

- In the filament making process, a compromise between surface roughness and oval cross-section must be found.

- In the 3D printing process, a correlation between nozzle temperature and printing speed have been verified.

- The obtained results expand the basic knowledge of PP based 3D printing technique, opening new interesting topics on the material formulations, such as increasing the talc content or try other fillers, and on the parameters optimisation for bigger objects.

References

[1] S. Singh, S. Ramakrishna, R. Singh, Material issues in additive manufacturing: A review, Journal of Manufacturing Processes 25 (2017) 185-200.

[2] T.D. Ngo, A. Kashani, G. Imbalzano, K.T.Q. Nguyen, D. Hui, Additive manufacturing (3D printing): A review of materials, methods, applications and challenges, Composites Part B: Engineering 143 (2018) 172-196.

[3] N.T. Brian, R. Strong, A.G. Scott, A review of melt extrusion additive manufacturing processes: I. Process design and modeling, Rapid Prototyping Journal 20(3) (2014) 192-204.

[4] M. Monzón, Z. Ortega, A. Martínez, F. Ortega, Standardization in additive manufacturing: activities carried out by international organizations and projects, The international journal of advanced manufacturing technology 76(5-8) (2015) 1111-1121.

[5] H. Krueger, Standardization for Additive Manufacturing in Aerospace, Engineering 3(5) (2017) 585.

[6] L. Warnung, S.-J. Estermann, A. Reisinger, Mechanical Properties of Fused Deposition Modeling (FDM) 3D Printing Materials, RTejournal-Fachforum für Rapid Technologien 2018(1) (2018).

[7] D. Popescu, A. Zapciu, C. Amza, F. Baciu, R. Marinescu, FDM process parameters influence over the mechanical properties of polymer specimens: A review, Polymer Testing 69 (2018) 157-166.

[8] Y. Song, Y. Li, W. Song, K. Yee, K.Y. Lee, V.L. Tagarielli, Measurements of the mechanical response of unidirectional 3D-printed PLA, Materials & Design 123 (2017) 154-164.

[9] M. Jin, R. Giesa, C. Neuber, H.W. Schmidt, Filament Materials Screening for FDM 3D Printing by Means of Injection-Molded Short Rods, Macromolecular Materials and Engineering 303(12) (2018) 1800507.

[10] R. Singh, H.K. Garg, Fused deposition modeling—a state of art review and future applications, Reference Module in Materials Science and Materials Engineering, Elsevier, 2016, pp. 1-20.

[11] Y. Jiang, J. Wu, J. Leng, L. Cardon, J. Zhang, Reinforced and toughened PP/PS composites prepared by Fused Filament Fabrication (FFF) with in-situ microfibril and shish-kebab structure, Polymer 186 (2020) 121971.

[12] M. Spoerk, J. Sapkota, G. Weingrill, T. Fischinger, F. Arbeiter, C. Holzer, Shrinkage and Warpage Optimization of Expanded-Perlite-Filled Polypropylene Composites in Extrusion-Based Additive Manufacturing, Macromolecular Materials and Engineering 302(10) (2017) 1700143.

[13] M. Spoerk, C. Savandaiah, F. Arbeiter, S. Schuschnigg, C. Holzer, Properties of glass filled polypropylene for fused filament fabrication, Proceedings of the ANTEC Anaheim (2017) 105-111.

[14] M. Heidari-Rarani, M. Rafiee-Afarani, A.M. Zahedi, Mechanical characterization of FDM 3D printing of continuous carbon fiber reinforced PLA composites, Composites Part B: Engineering 175 (2019) 107147.

[15] G. Sodeifian, S. Ghaseminejad, A.A. Yousefi, Preparation of polypropylene/short glass fiber composite as Fused Deposition Modeling (FDM) filament, Results in Physics 12 (2019) 205-222.

[16] P. Geng, J. Zhao, W. Wu, W. Ye, Y. Wang, S. Wang, S. Zhang, Effects of extrusion speed and printing speed on the 3D printing stability of extruded PEEK filament, Journal of Manufacturing Processes 37 (2019) 266-273.

[17] A.W. Gebisa, H.G. Lemu, Influence of 3D Printing FDM Process Parameters on Tensile properties of ULTEM, Procedia Manufacturing 30 (2019) 331-338.

[18] C. Duty, C. Ajinjeru, V. Kishore, B. Compton, N. Hmeidat, X. Chen, P. Liu, A.A. Hassen, J. Lindahl, V. Kunc, What makes a material printable? A viscoelastic model for extrusion-based 3D printing of polymers, Journal of Manufacturing Processes 35 (2018) 526-537.

[19] M. Katschnig, F. Arbeiter, B. Haar, G. van Campe, C. Holzer, Cranial Polypropylene Implants by Fused Filament Fabrication Advanced Engineering Materials 19(4) (2017) 1600676.

[20] K. Ilyes, N.K. Kovacs, A. Balogh, E. Borbas, B. Farkas, T. Casian, G. Marosi, I. Tomuta, Z.K. Nagy, The applicability of pharmaceutical polymeric blends for the fused deposition modelling (FDM) 3D technique: Material considerations-printability-process modulation, with consecutive effects on in vitro release, stability and degradation, European journal of pharmaceutical sciences : official journal of the European Federation for Pharmaceutical Sciences 129 (2019) 110-123.

[21] J. Savolainen, M. Collan, How Additive Manufacturing Technology Changes Business Models? – Review of Literature, Additive Manufacturing 32 (2020) 101070.

[22] M. Frank, S.B. Joshi, R.A. Wysk, RAPID PROTOTYPING AS AN INTEGRATED PRODUCT/PROCESS DEVELOPMENT TOOL AN OVERVIEW OF ISSUES AND ECONOMICS, Journal of the Chinese Institute of Industrial Engineers 20(3) (2003) 240-246.

[23] O.S. Carneiro, A.F. Silva, R. Gomes, Fused deposition modeling with polypropylene, Materials & Design 83 (2015) 768-776.

[24] N. Kumar, P.K. Jain, P. Tandon, P. Mohan Pandey, Experimental investigations on suitability of polypropylene (PP) and ethylene vinyl acetate (EVA) in additive manufacturing, Materials Today: Proceedings 5(2) (2018) 4118-4127.

[25] M. Jin, C. Neuber, H.-W. Schmidt, Tailoring polypropylene for extrusion-based additive manufacturing, Additive Manufacturing 33 (2020) 101101.

[26] T. Chapman, J. Gillespie Jr, R. Pipes, J.-A. Manson, J. Seferis, Prediction of process-induced residual stresses in thermoplastic composites, Journal of composite materials 24(6) (1990) 616-643.

[27] M. Spoerk, C. Holzer, J. Gonzalez-Gutierrez, Material extrusion-based additive manufacturing of polypropylene: A review on how to improve dimensional inaccuracy and warpage, Journal of Applied Polymer Science 137(12) (2020) 48545.

[28] R.A. Phillips, Macromorphology of polypropylene homopolymer tacticity mixtures, Journal of Polymer Science Part B: Polymer Physics 38(15) (2000) 1947-1964.

[29] D.B. Malpass, Introduction to industrial polyethylene: properties, catalysts, and processes, John Wiley & Sons, Hoboken, New Jersey, 2010.

[30] G. Spiegel, C. Paulik, Polypropylene Copolymers Designed for Fused Filament Fabrication 3D-Printing, Macromolecular Reaction Engineering 14(1) (2020) 1900044.

[31] C.A. Chatham, C.E. Zawaski, D.C. Bobbitt, R.B. Moore, T.E. Long, C.B. Williams, Semi-Crystalline Polymer Blends for Material Extrusion Additive Manufacturing Printability: A Case Study with Poly(ethylene terephthalate) and Polypropylene, Macromolecular Materials and Engineering 304(5) (2019) 1800764.

[32] M. Gahleitner, C. Tranninger, P. Doshev, Heterophasic copolymers of polypropylene: Development, design principles, and future challenges, Journal of Applied Polymer Science 130(5) (2013) 3028-3037.

[33] T.-M. Wang, J.-T. Xi, Y. Jin, A model research for prototype warp deformation in the FDM process, The International Journal of Advanced Manufacturing Technology 33(11-12) (2007) 1087-1096.

[34] M. Elbadawi, J. Rivera-Armenta, B. Cruz, Polymeric Additive Manufacturing: The Necessity and Utility of Rheology, Polymer Rheology, Intechopen, London, United Kingdom, 2018, pp. 43-63.

[35] C. Ajinjeru, V. Kishore, X. Chen, C. Hershey, J. Lindahl, V. Kunc, A.A. Hassen, C. Duty, Rheological survey of carbon fiber-reinforced high-temperature thermoplastics for big area additive manufacturing tooling applications, Journal of Thermoplastic Composite Materials (2019) 1-19.

[36] R.K. Gupta, Polymer and composite rheology, CRC Press, Boca Raton, Florida, 2000.

[37] I. Calafel, R. Aguirresarobe, M. Peñas, A. Santamaria, M. Tierno, J. Conde, B. Pascual, Searching for Rheological Conditions for FFF 3D Printing with PVC Based Flexible Compounds, Materials 13(1) (2020) 178.

[38] M. Spoerk, J. Gonzalez-Gutierrez, C. Lichal, H. Cajner, G.R. Berger, S. Schuschnigg, L. Cardon, C. Holzer, Optimisation of the adhesion of polypropylene-based materials during extrusion-based additive manufacturing, Polymers 10(5) (2018) 490.

[39] G.y. Shi, B. Huang, J.y. Zhang, Enthalpy of fusion and equilibrium melting point of the β-form of polypropylene, Die Makromolekulare Chemie, Rapid Communications 5(9) (1984) 573-578.

[40] Y. Jahani, Dynamic rheology, mechanical performance, shrinkage, and morphology of chemically coupled talc-filled polypropylene, Journal of Vinyl and Additive Technology 16(1) (2010) 70-77.

[41] J.-M. Piau, J.-F. Agassant, Rheology for polymer melt processing, Elsevier, Amsterdam, The Netherlands, 1996.

[42] A.V. Shenoy, Rheology of filled polymer systems, Springer Science & Business Media, Dordrecht, The Netherlands, 2013.

[43] H. Azizi, J. Faghihi, An investigation on the mechanical and dynamic rheological properties of single and hybrid filler/polypropylene composites based on talc and calcium carbonate, Polymer composites 30(12) (2009) 1743-1748.

[44] L.A. Castillo, S.E. Barbosa, N.J. Capiati, Influence of talc genesis and particle surface on the crystallization kinetics of polypropylene/talc composites, Journal of applied polymer science 126(5) (2012) 1763-1772.

[45] K. Shelesh-Nezhad, A. Taghizadeh, Shrinkage behavior and mechanical performances of injection molded polypropylene/talc composites, Polymer Engineering & Science 47(12) (2007) 2124-2128.

[46] Y. Ryu, J.S. Sohn, B.C. Kweon, S.W. Cha, Shrinkage Optimization in Talc- and Glass-Fiber-Reinforced Polypropylene Composites, Materials 12(5) (2019) 746.